Modification of *Rhodospirillum rubrum* Ribulose Bisphosphate Carboxylase with Pyridoxal Phosphate. 2. Stoichiometry and Kinetics of Inactivation†

William B. Whitman and F. Robert Tabita*

ABSTRACT: *Rhodospirillum rubrum* ribulose bisphosphate carboxylase contains two high affinity binding sites for pyridoxal phosphate and two catalytic sites per dimer. However, pyridoxal phosphate binding at only one site is sufficient for inactivation of both catalytic sites. In the presence of 20 mM bicarbonate, 10 mM magnesium, and pyridoxal phosphate, the rates of inactivation and Schiff base formation are pseudo-first-order and show saturation kinetics. These observations provide additional evidence that pyridoxal phosphate binds at the active site of the *R. rubrum* carboxylase. It is also proposed that the large subunit may contain regulatory as well as catalytic properties.

Studies of the molecular aspects of the regulation of ribulose bisphosphate carboxylase have largely been concerned with the role of the small subunit (Nishimura & Akazawa, 1974; Kung & Marsho, 1976). The small subunit, which is invariably associated with the enzyme from eucaryotes, is often absent from enzymes prepared from procaryotes (Jensen & Bahr, 1977). An example of a procaryotic ribulose bisphosphate carboxylase which lacks the small subunit is the enzyme from *Rhodospirillum rubrum*, which is a stable dimer of large, catalytic subunits (Tabita & McFadden, 1974b). Therefore, the enzyme from *R. rubrum* provides an excellent opportunity to study the regulatory properties of the catalytic subunit of ribulose bisphosphate carboxylase. An indication that the large catalytic subunit does in fact have regulatory properties came from the observation that, like the enzymes from higher plants, the *R. rubrum* enzyme is activated by preincubation in the presence of bicarbonate and magnesium (Tabita & McFadden, 1974a). In this work, additional support for this hypothesis was obtained. It has been possible to show that complete inactivation of the *R. rubrum* ribulose bisphosphate carboxylase by the nonphysiological inhibitor, pyridoxal phosphate, requires binding at only one of the two catalytic sites present per dimer. Therefore, the potential for regulation of the dimer's activity by ligand interaction at one of the subunits exists.

Experimental Procedures

Homogeneous *Rhodospirillum rubrum* ribulose 1,5-bisphosphate carboxylase was prepared as described (Whitman & Tabita, 1978). The purified enzyme was stored at 4 °C in 50 mM potassium phosphate buffer, pH 7.5, and 1 mM Na_2EDTA.[1] Prior to treatment with pyridoxal phosphate, aged enzyme was activated by a 3-h incubation with 10 mM dithiothreitol at 30 °C. The dithiothreitol was removed by dialyzing the enzyme twice against 50 mM potassium Mops, pH 7.5, and 1 mM Na_2EDTA and once against the same buffer containing 20 mM sodium bicarbonate and 10 mM magnesium acetate. Incubations with pyridoxal phosphate were performed in the dark or subdued light at 30 °C. For most experiments, the incubations were for at least 60 min. Pyridoxal phosphate treatment was terminated by the addition of the enzyme to the complete assay mixture containing 0.5 mM ribulose bisphosphate, 20 mM $NaH^{14}CO_3$, 10 mM magnesium acetate, 1 mM Na_2EDTA, and 40 mM potassium Mops, pH 7.5, in a total volume of 0.25, 0.50, or 1.0 mL. The assays were terminated and acid stable radioactivity determined as previously described (Whitman & Tabita, 1976). The specific activity of the enzyme is defined in μmol of CO_2 fixed per min per mg of enzyme.

Spectral Measurements. All spectra were recorded with a Beckman 25 dual beam spectrophotometer in raised-bottom, quartz microcuvettes containing 0.25–0.30 mL of the enzyme–pyridoxal phosphate solution at 30 °C. The extinction coefficients of pyridoxal phosphate at 5-nm intervals from 500 to 375 nm in 50 mM potassium Mops, pH 7.5, and 1 mM Na_2EDTA were calculated from the optical densities of two solutions of known concentration of pyridoxal phosphate. Similarly, the extinction coefficients of pyridoxal phosphate–poly(L-lysine) complex were determined with at least an 18-fold greater concentration of ε-amino groups than pyridoxal phosphate. The approximate extinction coefficient of the pyridoxal phosphate–enzyme complex was determined from the difference spectrum of the enzyme and the enzyme–pyridoxal phosphate complex in 50 mM potassium Mops, pH 7.5, 1 mM Na_2EDTA, 20 mM $NaHCO_3$, and 10 mM magnesium acetate. The concentration of enzyme was 21.6 μM, and the concentration of pyridoxal phosphate was 6.6 μM. Experimentally, the concentrations of the free and enzyme bound forms of pyridoxal phosphate were then estimated by fitting the extinction coefficients of the free and bound forms of pyridoxal phosphate to the difference spectrum of the enzyme and enzyme–pyridoxal phosphate complex from 500 to 375 nm. These calculations were performed by the CDC 6600 computer at the University of Texas at Austin using Program Linear of the EDSTATJ statistical package. The concentration of both forms of pyridoxal phosphate is then calculated directly from the "raw weight" of each spectrum which gave the best fit to the experimental spectrum.

Evaluation of the Rate Constants. For a two-step mechanism of inactivation of an enzyme by an inhibitor

$$E + I \underset{k_{-1}}{\overset{k_{+1}}{\rightleftharpoons}} E \cdot I \underset{k_{-2}}{\overset{k_{+2}}{\rightleftharpoons}} E\text{-}I$$

† From the Department of Microbiology, University of Texas at Austin, Austin, Texas 78712. *Received August 25, 1977.* This work was supported by National Science Foundation Grant No. PCM 74-10297, by Robert A. Welch Foundation Grant No. F-691, and by National Institutes of Health Grant No. GM-24497.

[1] Abbreviations used: EDTA, (ethylenedinitrilo)tetraacetic acid; Mops, 4-morpholinepropanesulfonic acid; PLP, pyridoxal 5′-phosphate.

0006-2960/78/0417-1288$01.00/0

where E is the unbound enzyme, I is the unbound inhibitor, E·I is a rapidly reversible enzyme–inhibitor complex, and E–I is a slowly reversible enzyme-inhibitor complex, the following equations can be written. If R is the fraction of total enzyme unbound and noncovalently complexed to pyridoxal phosphate at equilibrium (Chen & Engel, 1975), then

$$R = \frac{1 + \frac{k_{+1}}{k_{-1}}[I]}{1 + \frac{k_{+1}}{k_{-1}}[I] + \frac{k_{+1}k_{+2}}{k_{-1}k_{-2}}[I]}$$

and

$$\frac{1}{[I]} = \frac{k_{+1}k_{+2}}{k_{-1}k_{-2}}\left(\frac{1}{1-R}\right) - \left(1 + \frac{k_{+2}}{k_{-2}}\right)\frac{k_{+1}}{k_{-1}}$$

Furthermore, if $[E_T]$ is the total enzyme concentration and

$$F = \left(\frac{[E] + [E \cdot I]}{[E_T]}\right)^2$$

then

$$F^{1/2} = R$$

If k_{+2} is the rate-limiting step in the forward reaction, when [E–I] is small immediately after initiation of the reaction between enzyme and inhibitor, inactivation appears to be first order and irreversible (Piszkiewicz & Smith, 1971); then applying the treatment of Kitz & Wilson (1962)

$$\ln R = \frac{-k_{+2}t}{1 + \frac{k_{-1}}{k_{+1}[I]}}$$

and

$$\frac{1}{k_{obsd}} = \frac{1}{k_{+2}} + \frac{k_{-1}}{k_{+1}k_{+2}}\frac{1}{[I]}$$

However, if [E–I] is not small, inactivation appears first order and reversible. Then k_{obsd} is obtained from the slope of the plots of $-\ln (A_t - A_\infty)/(A_0 - A_\infty)$ vs. time, where A_t is either the fractional residual activity or the optical density at 380 nm at time t, and A_∞ and A_0 are at equilibrium and zero time, respectively. Replots of $1/k$ vs. $1/[I]$ yield $1/(k_2 + k_{-2})$ as the ordinate intercept (Amdur & Hammes, 1966). All linear plots are the least-square estimates calculated with a Wang 142 electronic calculator. Rate constants are presented ± one standard deviation.

For measurements at equilibrium, the concentration of free pyridoxal phosphate was calculated from the concentrations of total pyridoxal phosphate, enzyme, and the fractional residual activity (F) according to the equation

$$[PLP_{free}] = [PLP_{total}] - 2[E_T](1 - F^{1/2})$$

Results

The binding of pyridoxal phosphate to the *R. rubrum* ribulose bisphosphate carboxylase was quantitated by measuring the spectral changes of pyridoxal phosphate upon binding. These changes included a decrease in absorbance of unbound pyridoxal phosphate at 390 nm and an increase in absorbance of the bound pyridoxal phosphate at 415 and 340 nm (Whitman & Tabita, 1978). This method is preferable to measuring pyridoxal phosphate incorporation after sodium borohydride reduction because reduction inhibited the enzyme in the absence of pyridoxal phosphate. Because the enzyme is unstable at high protein concentrations, the optical density changes measured were very small, about 0.020 cm^{-1} at the lowest concentrations of pyridoxal used. Furthermore, the spectra of the unbound and enzyme bound forms of pyridoxal phosphate overlap so that the major absorbance changes include contributions of both forms of pyridoxal phosphate. Therefore, to improve the accuracy of measurements of binding, the spectra of the pyridoxal phosphate–enzyme complexes were fitted to the spectra of the bound and free forms of pyridoxal phosphate at 5-nm intervals from 375 to 500 nm by Program Linear from the computer library at the University of Texas at Austin. Spectra were not extended below 375 nm due to interference by the optical density changes of enzyme origin similar to those previously described (Rabin & Trown, 1964; Siegel & Lane, 1972).

TABLE I: Comparison between the Calculated Concentrations of the Bound and Unbound Forms of Pyridoxal Phosphate.[a]

PLP added (μM)	PLP bound[b] (μM)	PLP unbound[b] (μM)	PLP(calcd)/ PLP(added)[c]	PLP SB[b] (μM)	PLP(SB)/ PLP(bound)
8.81	8.09	1.04	1.04	4.45	0.550
16.1	15.5	1.89	1.08	8.57	0.553
21.7	20.7	5.58	1.21	11.5	0.556
35.5	25.6	10.4	1.01	14.2	0.555
42.7	29.5	17.7	1.11	16.4	0.556

[a] Conditions: as described in Experimental Procedures under spectral measurements. The enzyme concentration was 18.3 μM. [b] The concentrations of the bound, unbound, and Schiff base (SB) forms of pyridoxal phosphate were calculated by Program Linear as described in Experimental Procedures. [c] The calculated concentration of pyridoxal phosphate is the sum of the concentrations of the bound and unbound forms.

The validity of this method could be tested by comparing the total concentration of the free and bound forms of pyridoxal phosphate with the concentration of pyridoxal phosphate added (Table I). Over a five-fold concentration range of pyridoxal phosphate, the ratio of calculated pyridoxal phosphate to added pyridoxal phosphate was approximately constant, with an average value of 1.09. This indicates that the method slightly overestimates the concentration of pyridoxal phosphate. A likely explanation is that the spectrum for the bound form of pyridoxal phosphate was obtained under conditions which proved to be a sixfold excess of enzyme binding sites to pyridoxal phosphate. Under these conditions, some unbound pyridoxal phosphate would remain and cause a slight overestimation of the concentration of bound pyridoxal phosphate in the subsequent calculations. The concentration of the intramolecular hydrogen bonded Schiff base (415 nm absorbing material) can also be calculated from the extinction coefficients of pyridoxal phosphate and poly(L-lysine) mixtures. Over a fivefold concentration range of pyridoxal phosphate, the ratio of intramolecular hydrogen bonded Schiff base to total pyridoxal phosphate bound was constant (Table I). An average value for this ratio of 0.554 indicates that approximately 55% of the enzyme-bound pyridoxal phosphate is the intramolecular hydrogen-bonded Schiff base. The remainder is probably the 340-nm absorbing form of the enzyme-bound pyridoxal phosphate (Whitman & Tabita, 1978).

The Scatchard plots of the data in Table I indicated 1.9 ± 0.5 (± one standard deviation) high affinity pyridoxal phosphate binding sites per dimer. A similar result was obtained in two other experiments with enzyme from the same and one other purification. The apparent binding constants, determined from the slopes of the Scatchard plots, varied from 6.2 ± 1.7 × 10^4 to 4.6 ± 0.3 × 10^5 M^{-1}.

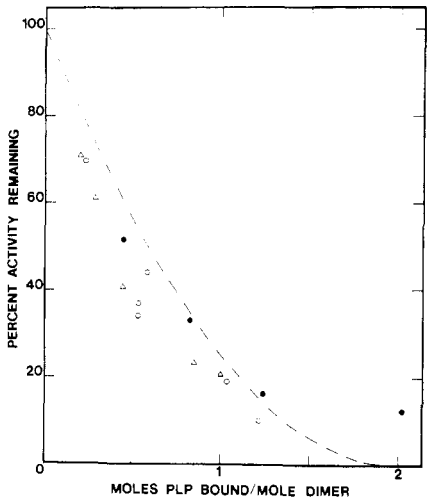

FIGURE 1: Stoichiometry of pyridoxal phosphate inactivation. Ribulose bisphosphate carboxylase was incubated with between 8 and 45 μM pyridoxal phosphate for at least 60 min and scanned with a Beckman 25 dual beam spectrophotometer at 30 °C. The concentration of bound pyridoxal phosphate was calculated from the spectrum as described in the Experimental Procedures. The symbols represent different experiments. (●) The enzyme concentration is 14.7 μM. Percent activity remaining was determined after diluting the enzyme 56-fold in buffer containing pyridoxal phosphate prior to a 10-min assay. The enzyme specific activity was 2.6. (△) The enzyme concentration was 21.4 μM. Percent activity remaining was determined after diluting the enzyme 50-fold in buffer prior to a 10-min assay. The enzyme specific activity was 1.3. (○) The enzyme concentration was 25.1 μM. Percent activity remaining was determined without dilution prior to a 1-min assay. The enzyme specific activity was 1.3.

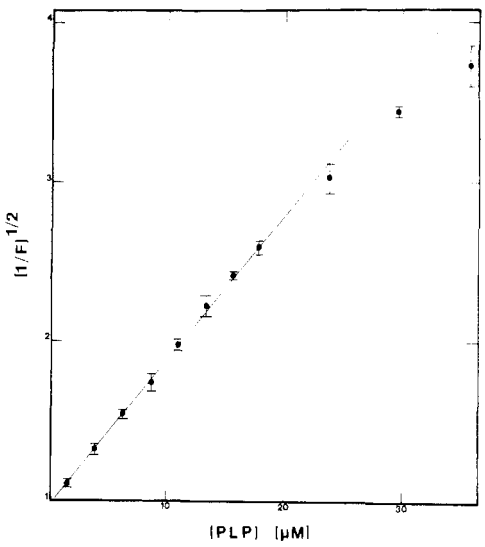

FIGURE 2: Stoichiometry of pyridoxal phosphate inactivation. The justification of the plot is given in the text. Enzyme, 2 μM, was incubated for at least 210 min at 30 °C in the presence of pyridoxal phosphate as described in Experimental Procedures. Enzyme activity was assayed in triplicate for 1 min. The enzyme specific activity was 3.4. The bars in the figure represent one standard deviation around the mean. The line is the least-squares estimate at pyridoxal phosphate concentrations below 18 μM.

When pyridoxal phosphate binding and inhibition of ribulose bisphosphate carboxylase activity were measured, the results shown in Figure 1 were obtained. By extrapolation of the curve to the abscissa at low concentrations of pyridoxal phosphate, a stoichiometry of inhibition of about one mole of pyridoxal phosphate bound per mole of dimer was obtained. However, by extrapolation at higher pyridoxal phosphate concentrations, a stoichiometry of 2 mol of pyridoxal phosphate per mol of dimer was obtained. This relationship was unchanged by assaying enzyme activity for 10 min in either the presence or absence of pyridoxal phosphate or for 1 min in the absence of pyridoxal phosphate. Two plausible models may account for this behavior. In the first, the dimer may contain one inhibitory site which binds pyridoxal phosphate at low concentrations and a second noninhibitory site which can also bind pyridoxal phosphate at high concentrations. In the second model, the dimer may contain two inhibitory sites of equal affinity for pyridoxal phosphate, but binding at either site is sufficient for complete inhibition of the dimer.

These two models may be distinguished. The first model suggests that, if:

$$E + P \rightleftharpoons EP \tag{1}$$

and

$$K_{app} = \frac{[EP]}{[E][P]} \tag{2}$$

where K_{app} is the apparent binding constant of the inhibitory site, [E] signifies the concentration of enzyme lacking PLP bound at the inhibitory site, [P] is the concentration of unbound pyridoxal phosphate, and [EP] is the concentration of enzyme with PLP bound at the inhibitory site; and

$$F = \frac{[E]}{[E_T]} \tag{3}$$

where F is the fractional residual activity determined in the presence of pyridoxal phosphate, and $[E_T]$ is the total enzyme concentration, then

$$\frac{1}{F} = [P]K_{app} + 1 \tag{4}$$

However, the second model suggests that if

$$K_{app} = \frac{[E_1P]}{[E_1][P]} = \frac{[E_2P]}{[E_1][P]} \tag{5}$$

where K_{app} is the apparent binding constant of either inhibitory site, and

$$F = \frac{[E_1]}{[E_T]}\frac{[E_2]}{[E_T]} = \left(\frac{[E]}{[E_T]}\right)^2 \tag{6}$$

or the fractional residual activity equals the concentration of enzyme not bound by pyridoxal phosphate at both sites when the sites have an equal affinity for pyridoxal phosphate, then

$$\left(\frac{1}{F}\right)^{1/2} = [P]K_{app} + 1 \tag{7}$$

When the ratio of pyridoxal phosphate to enzyme is high, the concentration of unbound pyridoxal phosphate, [P], is approximately equal to the total concentration of pyridoxal phosphate. Therefore, plots of either the reciprocal of the fractional residual activity (if the first model is correct) or the reciprocal of the square root of the fractional residual activity (if the second model is correct) vs. the pyridoxal phosphate concentration should be linear. Furthermore, the slope of the line should be equal to the apparent binding constant for pyridoxal phosphate. As shown in Figure 2, a plot of the reciprocal of the square root of the fraction of activity remaining vs. the pyridoxal phosphate concentration is linear up to 18 μM pyridoxal phosphate. Furthermore, a plot of the reciprocal of the fraction of activity remaining vs. pyridoxal phosphate for the same data is not linear (not shown). The apparent binding constant, K_{app}, obtained from the slope of the line is 9.1×10^4 M^{-1}, or within the range determined from the Scatchard plots

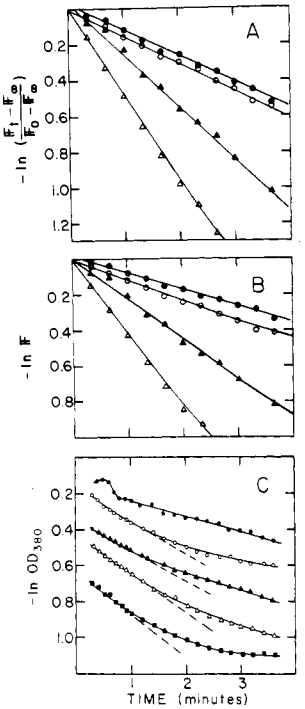

FIGURE 3: Pseudo-first-order rates of pyridoxal phosphate inactivation and binding. Conditions are described in the footnotes to Table II. (A) Plotted according to a reversible mechanism. (B) Plotted according to an irreversible mechanism. Lines are the least-square estimates of the linear portions of the curves. The concentrations of pyridoxal phosphate are: (●) 5.5 μM, (○) 8.1 μM, (▲) 16 μM, and (△) 33 μM. (C) Pseudo-first-order plots of the optical density change at 380 nm upon pyridoxal phosphate addition. The concentrations of pyridoxal phosphate used were: (●) 5.2 μM, (○) 10 μM, (▲) 16 μM, (△) 21 μM, and (■) 42 μM. The dashed lines are the least-square estimates of the linear portion of the curves. The units on the ordinate are arbitrary.

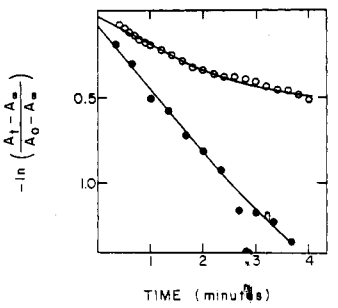

FIGURE 4: Comparison of the pseudo-first-order rate of inactivation and rate of change in the optical density at 380 nm. The optical density change was recorded with a Beckman 25 dual beam spectrophotometer at 30 °C. Other conditions were as described in Experimental Procedures. The enzyme concentration was 4.3 μM and had a specific activity of 3.3. The pyridoxal phosphate concentration was 12 μM. (○) The rate of change in the optical density. A is the optical density at 380 nm. (●) The rate of inactivation. A is the fractional residual activity after a 5-min assay.

when pyridoxal phosphate binding was measured directly. Moreover, when some of the data presented in Figure 1 was replotted according to eq 7, using the calculated concentration of free pyridoxal phosphate, the apparent binding constant obtained was identical with that obtained from the Scatchard plot.

The broken line in Figure 1 is the theoretical curve expected from the second model when the maximum number of high affinity pyridoxal phosphate binding sites per dimer is two. Clearly, the data obtained consistently fall below the theoretical line. The best explanation for this behavior is that the preparations of enzyme used contained slightly less than two pyridoxal phosphate binding sites per dimer, which may reflect the fact that the specific activity of the enzyme used in these experiments was less than maximal.

The deviation from linearity of plots of the reciprocal of the square root of the fractional residual activity vs. the concentration of pyridoxal phosphate at high concentrations of pyridoxal phosphate suggested that inactivation did not occur by a simple biomolecular reaction as described in eq 1. This effect can also be seen in the failure of high concentrations of pyridoxal phosphate to give complete inhibition of enzyme activity (Whitman & Tabita, 1978). However, the relative inhibition of the native enzyme over a 20-fold range in pyridoxal phosphate concentration is identical with the inhibition of the pyridoxal phosphate and sodium borohydride modified enzyme. Therefore, it is unlikely that either a fraction of the total enzyme is insensitive to pyridoxal phosphate or the pyridoxal phosphate-enzyme complexes retain partial activity. Furthermore, at low pyridoxal phosphate concentrations, the rate of inactivation is a pseudo-first-order process for up to 3.5 min (greater than 70% inhibition, Figure 3A). When the data was replotted as an irreversible reaction, Figure 3B, linear plots were obtained for the first minutes of the reaction but were curvilinear after 2 min for the highest concentrations of pyridoxal phosphate tested. Replots of the slopes of the linear portions of the curves indicated saturation kinetics.

Similar behavior has been described for the pyridoxal phosphate inactivation of glutamate dehydrogenase (Piszkiewicz & Smith, 1971; Chen & Engel, 1975) and has been interpreted as evidence for a two step mechanism of inactivation

$$E + P \underset{k_{-1}}{\overset{k_{+1}}{\rightleftharpoons}} E \cdot P \underset{k_{-2}}{\overset{k_{+2}}{\rightleftharpoons}} E\text{-}P \qquad (8)$$

where E and P represent the unbound forms of enzyme and pyridoxal phosphate, E·P is a noncovalent complex between the enzyme and pyridoxal phosphate, and E–P is the Schiff base between the enzyme and pyridoxal phosphate. The noncovalent complex dissociates upon dilution into the assay, which accounts for the failure to obtain complete inhibition at high pyridoxal phosphate concentrations.

Support for this mechanism with ribulose bisphosphate carboxylase was obtained by comparing the rate of pyridoxal phosphate inactivation with the rate of the optical density change which occurs upon binding (Figure 4). Under comparable conditions the pseudo-first-order rate in the loss of optical density at 380 nm was 0.163 ± 0.003 min^{-1} (± one standard deviation) while the rate of inactivation was 0.367 ± 0.017 min^{-1}. Therefore, the ratio of the rate of inactivation to the rate of the optical density change is 2.25, or very close to the expected ratio of 2 for the stoichiometry of pyridoxal phosphate inhibition. Furthermore, the rate of the initial loss in optical density at 380 nm (or increase in optical density at 415 nm, data not shown) indicated first-order irreversible kinetics (Figure 3C), and the replot of the slopes demonstrated saturation kinetics.

The mechanism described in eq 8 suggests that at equilibrium a linear relationship exists between the reciprocal of the pyridoxal phosphate concentration and the reciprocal of 1—the square root of the fractional residual activity (Chen & Engel, 1975). Thus, several independent measurements of the individual rate constants can be made from: the extent of inactivation at equilibrium, the rates of inactivation, and the rates of the optical density changes. These constants are presented in Table II.

It is evident that the two estimates of k_{+1}/k_{-1} and k_{-2} are close (Table II). However, k_{+1}/k_{-1} could not be estimated

TABLE II: Rate Constants for Pyridoxal Phosphate Inactivation of *Rhodospirillum rubrum* Ribulose Bisphosphate Carboxylase[a]

Constant	Constant[b]	Source[c]
$\frac{k_{+1}k_{+2}}{k_{-1}k_{-2}}$	$2.62 \pm 0.02 \times 10^5$ M^{-1}	Equilibrium
	$1.09 \pm 0.14 \times 10^5$ M^{-1}	Equilibrium[d]
$\frac{k_{+1}}{k_{-1}}$	$7.73 \pm 0.73 \times 10^4$ M^{-1}	Equilibrium
	$7.84 \pm 2.43 \times 10^4$ M^{-1}	Initial ΔOD
	$3.95 \pm 1.62 \times 10^4$ M^{-1}	Initial inact.[d]
	$4.08 \pm 1.91 \times 10^4$ M^{-1}	Equilibrium[d]
$\frac{k_{+2}}{k_{-2}}$	3.39 ± 0.32	Equilibrium
	2.67 ± 1.20	Equilibrium[d]
$k_{+2(\text{inact})}$	1.12 ± 0.46 min^{-1}	Initial inact.
	0.53 ± 0.21 min^{-1}	Initial inact.[d]
$k_{+2} + k_{-2(\text{inact})}$	1.56 ± 0.20 min^{-1}	Initial inact.
$k_{-2(\text{inact})}$	0.432 ± 0.502 min^{-1}	Initial inact.
	0.355 ± 0.052 min^{-1}	Initial inact. & equilibrium
$k_{+2(\text{binding})}$	0.338 ± 0.083 min^{-1}	Initial ΔOD
$k_{-2(\text{binding})}$	0.100 ± 0.26 min^{-1}	Initial ΔOD & equilibrium

[a] Conditions: As described in Experimental Procedures. Rate constants are for 30 °C in 50 mM potassium Mops, pH 7.5, 1 mM EDTA, 20 mM $NaHCO_3$, and 10 mM magnesium acetate. [b] The rate constants are for the mechanism of inactivation designated (eq 8) in the text and are given ± one standard deviation. [c] Obtained from replots described in Experimental Procedures of the data in Figure 3 plus additional data not shown. Measurements from initial inactivation and at equilibrium are from the same experiment. The initial inactivation means within the first 3.67 min of pyridoxal phosphate addition to the enzyme. At equilibrium means after at least 90 min, when no further inactivation could be detected. The enzyme concentration was 1.5 μM and had a specific activity of 3.3. Initial ΔOD refers to the initial rate of decrease in the optical density at 380 nm as described in the text. Conditions are identical with those described in Experimental Procedures. The enzyme concentration was 13.5 μM. [d] Rate constants for aged enzyme. The enzyme concentration was 1.2 μM and had a specific activity of 0.53.

from the replot of the initial ("irreversible") rate of inactivation. This is probably caused by partial reactivation of the Schiff base upon dilution of the enzyme into the assay, as would be expected from the estimates of k_{-2}(inactivation) of 0.432 and 0.355 min^{-1}. This problem was not observed with another preparation of enzyme of lower specific activity and a correspondingly slower rate for k_{-2} (Table II, footnote *d*). The estimates of k_{+1}/k_{-1} from replots of the change in optical density would not suffer from this artifact. However, the estimate of k_{+2}, 1.12 min^{-1}, obtained from the initial rates of inactivation is very close to the value calculated from $k_{+2} + k_{-2}$ and k_{+2}/k_{-2}, namely, 1.20 ± 0.20 min^{-1}. The ratio of the rate of inactivation, k_{+2}(inactivation), and the rate of the optical density change, k_{+2}(binding), is 3.55 ± 0.77. This is significantly greater than the expected ratio of 2 and may reflect the different conditions under which the inactivation and spectral measurements were performed, i.e., a ninefold difference in enzyme concentration.

It was previously noted that the apparent binding and rate constants for pyridoxal phosphate inactivation varied somewhat between different preparations of enzyme. These changes correlated fairly well with the specific activity of the enzyme. This can be demonstrated by comparing the rate constants for enzyme with a high specific activity and enzyme with a low specific activity obtained upon storage (Table II). Thus, a sixfold decrease in specific activity resulted in a 2.5-fold decrease in $k_{+1}k_{+2}/k_{-1}k_{-2}$ and a twofold decrease in k_{+1}/k_{-1}. However, the ratio, k_{+2}/k_{-2}, was relatively constant although k_{+2} decreased twofold. The correlation between specific activity and the rate constants for enzyme preparations of intermediate specific activity was also observed (data not shown).

Discussion

Pyridoxal phosphate has been shown to be a powerful inhibitor of *Rhodospirillum rubrum* ribulose bisphosphate carboxylase (Whitman & Tabita, 1978). From the pattern of protection against pyridoxal phosphate inhibition or binding offered by the substrates, known inhibitors, and possible effectors, it was concluded that pyridoxal phosphate forms a Schiff base at a lysyl residue at the active site of the enzyme (Whitman & Tabita, 1978). The fact that the *R. rubrum* carboxylase is a dimer of two large, catalytic type, subunits of identical molecular weight (Tabita & McFadden, 1974b) led to the expectation that 2 mol of pyridoxal phosphate per mol of dimer would be necessary for complete inhibition of enzyme activity. Indeed, Scatchard plots of pyridoxal phosphate binding indicated that there are two high affinity binding sites per dimer. Therefore, it was of interest that the binding of less than 2 mol of pyridoxal phosphate per dimer gave almost complete inhibition of enzyme activity.

Plots of the reciprocal of the square root of the fractional residual activity vs. the pyridoxal phosphate concentration were linear at low pyridoxal phosphate concentrations. The deviation from linearity at high pyridoxal phosphate concentrations could be explained by a two-step mechanism of inactivation of the type shown to occur with the *R. rubrum* carboxylase and pyridoxal phosphate. Therefore, the dimer must contain two pyridoxal phosphate inactivation sites, and pyridoxal phosphate binding at either site is sufficient for complete loss of activity. These conclusions are supported by the observation that the pseudo-first-order rate of inactivation is twice the rate of pyridoxal phosphate binding as measured by the loss in optical density at 380 nm. This demonstrates that there are in fact two catalytic sites per dimer and that pyridoxal phosphate binding at one inactivation site inhibits both catalytic sites. Because the replots of the extent of inactivation at equilibrium are sensitive to the stoichiometry assumption, the agreement between the determinations of the rate constants for pyridoxal phosphate inactivation at equilibrium and during the initial inactivation confirms the stoichiometry of inactivation.

Finding one pyridoxal phosphate binding site per subunit of the *R. rubrum* carboxylase is consistent with the results obtained by Paech et al. (1977) for the pyridoxal phosphate inactivation of spinach ribulose bisphosphate carboxylase. These workers found 9.5 mol of high affinity pyridoxal phosphate binding sites per mol of hexadecameric enzyme, presumably at one pyridoxal phosphate binding site per catalytic subunit. Schloss & Hartman (1977) found that the incorporation of 0.4 mol of the active-site-directed reagent, 3-bromo-1,4-dihydroxy-2-butanone 1,4-bisphosphate, per mol of *R. rubrum* carboxylase subunits was sufficient for almost complete inactivation. Furthermore, Hartman et al. (1973) found that the incorporation of between 2 and 4 mol of the same reagent was sufficient for almost complete inactivation of the spinach ribulose bisphosphate carboxylase. Like pyridoxal phosphate, 3-bromo-1,4-dihydroxy-2-butanone, 1,4-bisphosphate inactivated by modifying lysyl residues of both the *R. rubrum* and spinach enzymes (Schloss & Hartman, 1977; Norton et al., 1975). Whether or not the active-site lysyl residues of the spinach and *R. rubrum* carboxylase are found in similar environments remains to be determined.

Evidence that inactivation by pyridoxal phosphate occurs

upon covalent bond formation was obtained by showing saturation kinetics for both inactivation and the optical density changes which occur upon pyridoxal phosphate binding. The association constant for the *R. rubrum* ribulose bisphosphate carboxylase and pyridoxal phosphate ($k_1k_2/k_{-1}k_{-2}$ = 2.62 $\times 10^5$ M^{-1}) is unusually high for an enzyme in which pyridoxal phosphate has no functional significance and is nearly as large as the association constant for the apotryptophanase from *Bacillus alvei* under similar conditions (Isom & DeMoss, 1975). When the individual rate constants were measured, it was apparent that the major determinant of the specificity of pyridoxal phosphate binding must be formation of the noncovalent complex prior to Schiff base formation. This is seen by comparing K_1 for formation of the noncovalent complex ($K_1 = k_{+1}/k_{-1}$ = 7.73 $\times 10^4$ M^{-1}) with K_2 for formation of the Schiff base ($K_2 = k_{+2}/k_{-2}$ = 3.39). Indeed, K_1 is about 10-fold greater than the association constant between pyridoxamine phosphate and serine apodehydratase (Schonbeck et al., 1975b). However, K_2 is almost 10^4-fold lower than the analogous binding constant with serine dehydratase but within the range found in other protein modification studies (Chen & Engel, 1975; Murphy, 1977). Furthermore, the individual rate constants for Schiff base formation were, for the forward reaction, k_{+2} = 0.34 min^{-1}, and, for the reverse reaction, k_{-2} = 0.10 min^{-1}. The rate constant for the reverse reaction is very close to that obtained for the dissociation of the Schiff base between pyridoxal phosphate and 6-aminocaproic acid at pH 7.8 and 25 °C, k_{-1} = 0.11 min^{-1} (Schonbeck et al., 1975a). Paech et al. (1977) have suggested that the high affinity of the active site of the spinach carboxylase for pyridoxal phosphate may be due to the presence of a low p*K* lysyl residue involved in carbon dioxide binding. However, an alternate explanation for an enhancement of Schiff base formation at neutral pH may be a proximity effect due to juxtaposing a pyridoxal phosphate close to the reactive lysyl residue in the noncovalent complex.

If pyridoxal phosphate is indeed an active-site-directed reagent, some features of the active site important for pyridoxal phosphate binding may be important for enzyme activity as well. When comparing high with low specific activity enzyme obtained upon storage of the homogeneous enzyme, a twofold decrease in the association constant for the noncovalent complex and the pseudo-first-order rate constant for Schiff base formation is observed. Because the ratio of the rate of formation and dissociation of the Schiff base remains relatively constant, the rate of dissociation of the Schiff base of low specific activity enzyme must also decrease. This also stresses the importance of publishing the specific activity of the enzyme preparations used for subsequent inactivation studies, particularly ribulose bisphosphate carboxylase.

We have previously demonstrated that pyridoxal phosphate acts at the active site of the *R. rubrum* ribulose bisphosphate carboxylase (Whitman & Tabita, 1976, 1978). It is consistent with this hypothesis that activation of the enzyme with bicarbonate and magnesium increases its affinity for pyridoxal phosphate and that enzyme preparations with a lowered specific activity have a lowered affinity for pyridoxal phosphate. Further support was also gained by demonstrating the presence of two pyridoxal phosphate inactivation sites and two catalytic sites per dimer. Therefore, it is intriguing that pyridoxal phosphate binding at only one of the inactivations sites is sufficient for inactivation of both catalytic sites. This does not appear to be a property peculiar to pyridoxal phosphate inactivation because the active-site-directed reagent, 3-bromo-1,4-dihydroxy-2-butanone, 1,4-bisphosphate, appears to show a similar mode of inactivation (Schloss & Hartman, 1977). Thus, the *R. rubrum* carboxylase may possess a hitherto unsuspected regulatory potential in the large, catalytic subunit. Whether or not this proves to be the case for more physiological inhibitors or activators remains to be tested. While the *R. rubrum* enzyme has a quaternary structure unique among the several ribulose bisphosphate carboxylases that have been isolated, the biological properties of the *R. rubrum* enzyme appear to be similar to those of the higher plant enzymes (Tabita & McFadden, 1974a,b; McFadden, 1974). The only established exception to this is its insensitivity to 6-phosphogluconate (Tabita & McFadden, 1972). Therefore, there is no a priori reason to assume that a similar regulatory potential in the large subunits of the higher plant enzyme will not be found.

Acknowledgments

We thank Lester R. Martin for assistance with the computer analysis, John E. Rogers for helpful discussions, and Esmond E. Snell for critically reading the manuscripts prior to publication.

References

Amdur, I., & Hammes, G. G. (1966) *Chemical Kinetics,* p 12, McGraw-Hill, New York, N.Y.

Chen, S.-S., & Engel, P. C. (1975) *Biochem. J. 147,* 351.

Hartman, F. C., Welch, M. H., & Norton, I. L. (1973) *Proc. Natl. Acad. Sci. U.S.A. 70,* 3721.

Isom, H. C., & DeMoss, R. D. (1975) *Biochemistry 14,* 4291.

Jensen, R. G., & Bahr, J. T. (1977) *Annu. Rev. Plant Physiol. 28,* 379.

Kitz, R., & Wilson, I. B. (1962) *J. Biol. Chem. 237,* 3245.

Kung, S. D., & Marsho, T. V. (1976) *Nature (London) 259,* 325.

McFadden, B. A. (1974) *Biochem. Biophys. Res. Commun. 60,* 312.

Murphy, A. J. (1977) *Arch. Biochem. Biophys. 180,* 114.

Nishimura, M., & Akazawa, T. (1974) *Biochem. Biophys. Res. Commun. 59,* 584.

Norton, I. L., Welch, M. H., & Hartman, F. C. (1975) *J. Biol. Chem. 250,* 8062.

Paech, C., Ryan, F. J., & Tolbert, N. E. (1977) *Arch. Biochem. Biophys. 179,* 279.

Piszkiewicz, D., & Smith, E. L. (1971) *Biochemistry 10,* 4544.

Rabin, B. R., & Trown, P. W. (1964) *Proc. Natl. Acad. Sci. U.S.A. 51,* 497.

Schloss, J. V., & Hartman, F. C. (1977) *Biochem. Biophys. Res. Commun. 75,* 320.

Schonbeck, N. D., Skalski, M., & Shafer, J. A. (1975a) *J. Biol. Chem. 250,* 5343.

Schonbeck, N. D., Skalski, M., & Shafer, J. A. (1975b) *J. Biol. Chem. 250,* 5359.

Siegel, M. I., & Lane, M. D. (1972) *Biochem. Biophys. Res. Commun. 48,* 508.

Tabita, F. R., & McFadden, B. A. (1972) *Biochem. Biophys. Res. Commun. 48,* 1153.

Tabita, F. R., & McFadden, B. A. (1974a) *J. Biol. Chem. 249,* 3453.

Tabita, F. R., & McFadden, B. A. (1974b) *J. Biol. Chem. 249,* 3459.

Whitman, W., & Tabita, F. R. (1976) *Biochem. Biophys. Res. Commun. 71,* 1034.

Whitman, W. B., & Tabita, F. R. (1978) *Biochemistry 17* (preceding paper in this issue).